(12)

Carderock Division
Naval Surface Warfare Center
Bethesda, MD 20084–5000

CARDEROCKDIV–92/011 September 1992
Ship Hydromechanics Department
Research and Development Report

Postswirl Propulsors – A Design Method and An Application

by
Benjamin Y.–H. Chen

Main text was presented at the International Symposium on Propulsors and Cavitation, Hamburg, Germany, 22–26 June 1992.

THIS PAGE INTENTIONALLY LEFT BLANK

REPORT DOCUMENTATION PAGE

1a. REPORT SECURITY CLASSIFICATION UNCLASSIFIED	1b. RESTRICTIVE MARKINGS
2a. SECURITY CLASSIFICATION AUTHORITY	3. DISTRIBUTION/AVAILABILITY OF REPORT Approved for public release; distribution is unlimited.
2b. DECLASSIFICATION/DOWNGRADING SCHEDULE	
4. PERFORMING ORGANIZATION REPORT NUMBER(S) CARDEROCKDIV-92/011	5. MONITORING ORGANIZATION REPORT NUMBER(S)
6a. NAME OF PERFORMING ORGANIZATION Carderock Division Naval Surface Warfare Center 6b. OFFICE SYMBOL (*If applicable*) Code 1544	7a. NAME OF MONITORING ORGANIZATION
6c. ADDRESS (*City, State, and ZIP Code*) Bethesda, Maryland 20084–5000	7b. ADDRESS (*City, State, and ZIP Code*)
8a. NAME OF FUNDING/SPONSORING ORGANIZATION Advanced Surface Machinery Program 8b. OFFICE SYMBOL (*If applicable*) Code 27B	9. PROCUREMENT INSTRUMENT IDENTIFICATION NUMBER
8c. ADDRESS (*City, State, and ZIP Code*) Propulsion and Auxiliary Systems Department David Taylor Model Basin Bethesda, Maryland 20084–5000	10. SOURCE OF FUNDING NUMBERS PROGRAM ELEMENT NO. 63724N PROJECT NO. WX22011 TASK NO. R0829–802 WORK UNIT ACCESSION NO.
11. TITLE (*Include Security Classification*) Postswirl Propulsors – A Design Method and An Application	
12. PERSONAL AUTHOR(S) Chen, Benjamin Y.–H.	
13a. TYPE OF REPORT Final 13b. TIME COVERED FROM_____TO_____	14. DATE OF REPORT (*YEAR, MONTH, DAY*) 1992, September 15. PAGE COUNT 28
16. SUPPLEMENTARY NOTATION Main text was presented at the International Symposium on Propulsors and Cavitation, Hamburg, Germany, 22–26 June 1992	
17. COSATI CODES FIELD / GROUP / SUB–GROUP	18. SUBJECT TERMS (*Continue on reverse if necessary and identify by block number*) Postswirl propulsors, mass conservation, momentum conservation, circulation conservation, hub effects.

19. ABSTRACT (*Continue on reverse if necessary and identify by block number*)

A design method for postswirl (PS) propulsors is addressed. The principles of momentum, mass, and circulation conservation are satisfied and the effects of the hub boundaries have been taken into account in the design and analysis methods. A PS propulsor was designed for close–to–uniform flow at the operating point for a surface ship. Self–propulsion experimental results show that the performance predictions agree well with the measurements.

20. DISTRIBUTION/AVAILABILITY OF ABSTRACT ☒ UNCLASSIFIED/UNLIMITED ☐ SAME AS RPT ☐ DTIC USERS	21. ABSTRACT SECURITY CLASSIFICATION UNCLASSIFIED
22a. NAME OF RESPONSIBLE INDIVIDUAL Benjamin Y.–H. Chen	22b. TELEPHONE (*Include Area Code*) (301) 227–1450 22c. OFFICE SYMBOL Code 1544

CONTENTS

FIGURES

FIGURES (Continued)

TABLES

NOMENCLATURE

c/D	Chord to diameter ratio
C_D	Drag coefficient
C_f	Skin friction coefficient
C_{Th}	Thrust loading coefficient
D_r	Rotor diameter
D_s	Stator diameter
EAR	Expanded area ratio
f	Ratio of stator radius to rotor radius
f_m/c	Maximum camber to chord length ratio
G	Nondimensional circulation
i	Component
i_t/D	Total rake to diameter ratio
K_Q	Torque coefficient
K_T	Thrust coefficient
m	Control point
N_r	Rotor RPM
P/D	Pitch to diameter ratio
q	Torque ratio, $q = Q_2/Q_1$
Q	Torque
r	Rotor
R_T	Bare hull resistance
s	Stator
t	Thrust deduction fraction
t/c	Thickness to chord ratio
T	Thrust
u_t	Tangential induced velocity
u_x	Axial induced velocity
u_{xii}, u_{tii}	Axial and tangential self–induced velocity for the i^{th} component
u_{xij}, u_{tij}	Axial and tangential velocity induced by the j^{th} component on the i^{th} component
V_t	Tangential inflow velocity
V_x	Axial inflow velocity

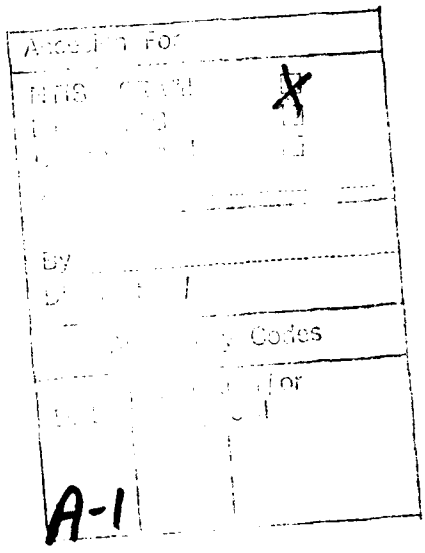

NOMENCLATURE (Continued)

$w_c(X_R)$	Circumferential mean wake fraction
w_T	Propulsor effective wake fraction
$w_x(X_R)$	Local wake fraction
x	Axial separation between the rotor and stator
X_R	Nondimensional radius measured from the shaft axis
X_{Rh}	Nondimensional hub radius
Z	Blade number
βi	Hydrodynamic pitch angle
θs	Skew angle
ω	Angular velocity
Γ	Circulation
λ	Lagrange multiplier

Subscripts: i = 1, 2
j = 1, 2
1 – rotor
2 – stator

All other notations in this report are in accordance with the International Towing Tank Conference (ITTC) Standard Symbols.*

* "International Towing Tank Conference Standard Symbols 1976," The British Ship Research Association, BSRA Technical Memorandum No. 500 (May 1976).

POSTSWIRL PROPULSORS - A DESIGN METHOD AND AN APPLICATION

by

Benjamin Y.-H. Chen

Carderock Division, Naval Surface Warfare Center, Bethesda, MD 20084-5000, U.S.A.

ABSTRACT

A design method for postswirl (PS) propulsors is addressed. The principles of momentum, mass, and circulation conservation are satisfied and the effects of the hub boundaries have been taken into account in the design and analysis methods. A PS propulsor was designed for close-to-uniform flow at the operating point for a surface ship. Self-propulsion experimental results show that the performance predictions agree well with the measurements.

INTRODUCTION

There has been a renewed interest in finding more efficient and quieter propulsors for new naval surface ships. A promising candidate is a postswirl (PS) propulsor which consists of a stator installed behind a rotor. One of the earliest work for PS propulsors was developed by Wagner [1]. PS propulsors exhibit many advantages in terms of powering and cavitation over single rotation (SR) propellers.

The improvements in the propulsive efficiency for the PS propulsor are due to the following reasons:

1. Reduced rotation losses in the propeller slipstream.
2. Reduced axial kinetic energy losses in the propeller slipstream.

The first improvement gain results from the fact that the tangential velocity generated by the stator is opposite to that generated by the rotor on the stator plane. The second source comes about because the stator causes the maximum rotor blade loading to shift inboard. This only occurs when the propulsor operates in a non-uniform flow.

The improvements in the cavitation inception speed for the PS propulsor result for the following reasons.

1. Reduced blade loading for blade surface cavitation.
2. Reduced tip circulation for tip vortex cavitation.

The first item is due to the stator blades taking some of the loading from the rotor blades. The second item is owing to a shift of the maximum rotor blade loading inboard.

The purpose of the present study was to develop a design method for the PS propulsor based on rational hydromechanics using the principles of momentum, mass, and circulation conservation. The method accommodates non-zero loading at the blade roots in the design and analysis process and accounts for the effects of the hub boundaries.

A PS propulsor was designed for close-to-uniform flow at the operating point for a surface ship. Self-propulsion measurements for the PS propulsor design are given.

A DESIGN METHOD FOR POSTSWIRL PROPULSORS

DESIGN PRINCIPLE

Momentum conservation requires that the PS propulsor generate a net force to overcome two types of drag; the bare body drag and the drag due to propulsor-hull interaction. There are two types of propulsor-hull interactions; thrust deduction and wake fraction, but only thrust deduction affects momentum conservation. Thrust deduction, an additional drag, results from the propulsor accelerating the local flow field about the ship and causing a reduction of the local hull surface pressure. In addition, the wall shear stress increases due to a higher velocity which in turn increases the frictional resistance. The thrust deduction fraction for propulsors is defined by

$$t = \frac{T - R_T}{T} \tag{1}$$

where R_T is the bare-hull resistance and T is the total thrust for all propulsors.

Using Lagally's theorem, Weinblum [2] developed a procedure to calculate thrust deduction. Cox and Hansen [3] developed a procedure of thrust deduction for a single rotation(SR) propeller in terms of the potential flow about the hull and appendages which are represented by surface singularity distributions. However, the thrust deduction factor for PS propulsors is still a research topic because of the complex interactions between the rotor and the stator. Since there is no thrust deduction measurement for the PS propulsor in the current study, the thrust deduction factor for SR propellers is employed in the present design method. When the thrust deduction value for a PS propulsor is measured on the proper hull form, it would be appropriate to use the thrust deduction for the PS propulsor.

Mass conservation determines the circulation distribution of the stator once the circulation distribution of the rotor is specified. Based on mass conservation, the preliminary diameter of the stator, D_s, can be determined from the rotor diameter, D_r, through the following formula.

$$D_s = f \times D_r \tag{2}$$

where

$$f = \left(\frac{\int_{X_{Rhr}}^{1}(V_{xr} + u_{xrr} + u_{xrs})X_{Rr}dX_{Rr}}{\int_{X_{Rhs}}^{1}(V_{xs} + u_{xss} + u_{xsr})X_{Rs}dX_{Rs}}\right)^{\frac{1}{2}} \tag{3}$$

where V_{xr} and V_{xs} are the axial inflow velocities for the rotor and the stator. u_{xrr} and u_{xss} are the axial self-induced velocities of the individual components. u_{xrs} and u_{xsr} are the axial velocity induced by the stator on the rotor and vice versa. X_R is the local radius of the individual components. X_{Rhr} and X_{Rhs} are the radii of the rotor and stator at the hub.

To determine the final stator diameter, It is required that the tip vortices generated by the rotor blades shall not impinge on the stator blades. In other words, there should not be large velocity gradients over the tips of the stator blades so that the stator will not operate in the tip vortices from the rotor. To be on the safe side, the final stator diameter should be selected so as to be smaller than the preliminary stator diameter determined based on mass conservation.

Circulation conservation determines the magnitude of the stator circulation once the magnitude of the rotor circulation is specified. In other words, the magnitude of the stator circulation has to be calculated such that the total circulation is conserved.

DESIGN PROCEDURE

A flow chart of the design method for PS propulsors, which is similar to that for contrarotating propellers (see Chen and Reed [4]), is shown in Figure 1. It consists of three phases: specification of operating conditions, design and analysis.

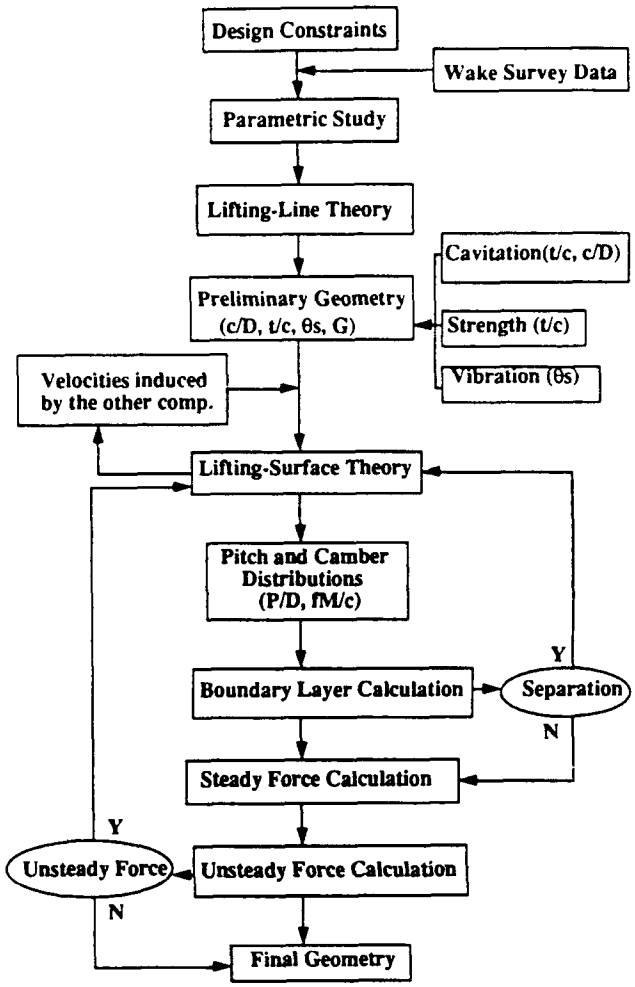

Fig. 1. Flow chart of PS propulsor design method.

Specification of Operating Conditions

In the first phase, the design requirements and the wake survey data need to be provided. The effects of the hull on the flow and hull-propulsor interaction are traditionally represented by the nominal wake and two interaction coefficients; the thrust deduction factor described previously and the wake fraction.

The wake fraction results from having the propulsor operate in the spatially non-uniform wake field of the hull. This non-uniform wake mainly results from the shaft inclination and boundary layer growth along the hull. The same propulsor model can be operated in uniform flow at the same angular velocity and the advance speed varied until the thrust agrees with that measured behind the hull. The difference between the ship and thrust-identity speeds can be expressed as the Taylor wake fraction

$$w_T = 1 - \frac{V_A}{V_s} \tag{4}$$

where V_A is the advance speed and V_s the ship speed.

The wake at the location of the propulsor in the absence of the propulsor is called the nominal wake. The effective wake distribution determined in the presence of the propulsor depends on the mutual interaction of the propulsor and the stern boundary layer. In the design of a wake-adapted propulsor, the radial distribution of effective wake is traditionally represented by

$$(1 - w_x(X_R)) = \frac{1 - w_T}{1 - w_v}(1 - w_c(X_R)) \qquad (5)$$

where $(1 - w_c(X_R))$ is the nondimensional circumferential mean axial velocity component (nominal wake) from the wake survey, $1 - w_T$ is the Taylor wake and $1 - w_v$ the volumetric mean nominal wake.

Huang et al.[5] developed a theoretical calculation of the effective wake by solving a simplified Euler equation in a conservative force field. Moreover, Shih [6] solved the Euler equation in a non-conservative force field to predict the velocity distribution of a propeller operating in an inviscid, axisymmetric shear flow. Results of both theoretical predictions from Huang et al. and Shih show good agreement with experimental data. However, the calculation of the effective wake for PS propulsors is still beyond the state-of-the-art due to the complex interactions between the PS propulsor and the hull, and between the rotor and the stator. In the present design procedure, the method for calculating the effective wake for a SR propeller is employed.

Design

In the design phase, there are three design stages; preliminary, intermediate, and final.

Preliminary Design

In the preliminary design stage, one investigates a limited number of design parameters such as diameter, angular velocity, number of blades and radial distribution of loading. In general, lifting-line theory can economically determine an optimum design through a large number of parametric studies from the calculations of efficiency, strength, and cavitation. Economy of effort is especially crucial for the PS propulsor design because of the large number parameters as well as the calculation of mutual interactions between the rotor and the stator.

Kerwin et al. [7] developed an advanced lifting-line theory for PS propulsors. A vortex lattice method was used to solve the lifting-line theory. The induced velocities in the theory include the self-induced velocities of each blade row as well as the velocities induced by the other blade row. A velocity diagram for PS propulsors is given in Figure 2.

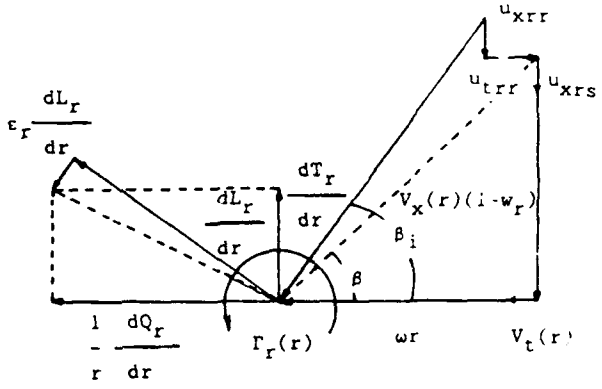

(a) Rotor.

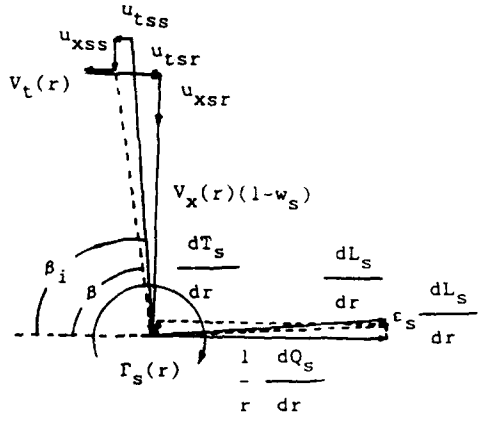

(b) Stator.

Fig. 2. Velocity diagram for PS propulsors.

Some highlights of Kerwin et al.'s theory are described in the following. Three fundamental assumptions are adopted:

1. The blades of each blade row are represented by straight, radial lifting lines.
2. The blades of each blade row are considered to have equal angular spacing and identical loading.
3. The wake geometry is assumed to be purely helical, with the pitch at each radius determined either by the undisturbed inflow (linear or lightly loaded theory), or by the induced flow at the lifting line (moderately loaded theory).

Based on a thrust identity (it can also be represented by a torque identity), Kerwin et al. obtained the optimum circulation using a variational approach. In other

words, for a prescribed total thrust, T, and a prescribed torque ratio, q, between the two blade rows, the optimum circulation of each blade row can be obtained by minimizing the total power.

The variational approach develops as follows. Blade row 1 represents the rotor and blade row 2 represents the stator.

Minimize

$$\omega_1 Q_1 + \omega_2 Q_2, \tag{6}$$

subject to the constraints:

$$T_1 + T_2 - T = 0, \tag{7}$$

and

$$Q_2 - qQ_1 = 0. \tag{8}$$

A constrained objective function is formed:

$$H = \omega_1 Q_1 + \omega_2 Q_2 + \lambda_1(T_1 + T_2 - T) + \lambda_2(Q_2 - qQ_1), \tag{9}$$

where ω_1 and ω_2 are the angular velocities for each blade row, λ_1 and λ_2 are Lagrange multipliers, T_1 and T_2 are the thrusts for each blade row, and Q_1 and Q_2 are the torques for each blade row. Thrusts and torques are computed using the following formulas:

$$T_i = \rho \sum_{m=1}^{M_i} Z_i \Gamma_{im} \Delta X_{Rim} (V_{tim} + \omega_i X_{Rim} + u_{tim}) \qquad (i = 1, 2), \tag{10}$$

and

$$Q_i = \rho \sum_{m=1}^{M_i} Z_i \Gamma_{im} \Delta X_{Rim} X_{Rim} (V_{xim} + u_{xim}) \qquad (i = 1, 2). \tag{11}$$

where X_{Rim} is the local radius from the shaft axis to the control point, m, ΔX_{Rim} is the radial distance between the two lattice points surrounding control points m, Z_i is the number of blades and M_i the number of control points. Γ_{im} is the circulation, V_{xim} and V_{tim} are the axial and the tangential inflow velocities, and u_{xim} and u_{tim} are the axial and the tangential induced velocities at the control points. These induced velocities include the self-induced velocities and the velocities induced by the other blade row. The velocities u_{xim} and u_{tim} can be expressed as follows.

$$u_{xim} = \sum_{j=1}^{2} \sum_{n=1}^{M_j} \Gamma_{jn} u_{xim,jn} \qquad (i = 1, 2), \tag{12}$$

and

$$u_{tim} = \sum_{j=1}^{2} \sum_{n=1}^{M_j} \Gamma_{jn} u_{tim,jn} \qquad (i = 1, 2), \tag{13}$$

where $u_{xim,jn}$ and $u_{tim,jn}$ stand for the influence functions for the axial and the tangential velocities induced on the control point, m, of the ith component by a nth element of unit strength on the jth component. The influence functions represent the self-induced velocities when i equals j and the mutual interaction velocities when i does not equal j.

The constrained objective function H, Eq (9), is expanded from Eqs. (10), (11), (12), and (13) and its partial derivatives with respect to the unknown circulations, Γ_{ii}, and Lagrange multipliers, λ_i, are set equal to zero. This process provides $M_1 + M_2 + 2$ equations which can be solved for the circulations at the control points and the Lagrange multipliers. That is to say, one obtains

$$\frac{\partial H}{\partial \Gamma_{ii}} = 0 \qquad (i = 1, ..., M_i, i = 1, 2), \tag{14}$$

and

$$\frac{\partial H}{\partial \lambda_i} = 0 \qquad (i = 1, 2). \tag{15}$$

The optimum circulation distribution in Kerwin et al.'s theory allows non-zero loading at the blade roots which is an important factor for PS propulsors. The theory provides an equal and opposite circulation for the rotor and the stator at the hub to ensure minimum hub vortex strength. In other words, the net circulation for the two individual blade rows at the hub is zero. Therefore, the present design procedure accounts for the effects of the hub boundaries. In addition, the slope of the circulation, $\frac{d\Gamma}{dr}$, is constrained to be essentially zero at the hub so that the trailing vortex sheet in the hub region may be "eliminated".

The optimum circulations for a SR propeller between the Kerwin et al. and the Caster et al.[8]'s programs were compared in Chen et al.[9]. The results from Kerwin et al.'s program are very good. This indicates that the variational method is an appropriate approach to solve lifting-line theory. However, this does not indicate that Kerwin et al.'s program is an adequate tool to design PS propulsors unless it can be validated. This validation is part of the effort pursued in the present study.

The real flow passing through the rotor and the stator can be envisioned as an unsteady flow both in time and space because of the different blade numbers and rotation speeds. However, as is usually done, the design problem is simplified by the use of circumferential-average inflow. Calculating the mutual interaction velocities is one of the most critical factors affecting the PS propulsor design. To obtain accurate mutual interaction velocities, the use of the interaction velocities calculated from lifting-surface theory developed by Chen and Reed [10] is employed in the present study.

Intermediate Design

In the intermediate design stage, cavitation and strength are major concerns. Blade surface cavitation results in blade erosion, noise, and thrust loss which are detrimental to ship performance. In order to improve the cavitation performance, one can vary blade thickness, chord distribution, and blade loading. However, the strength and the propulsive performance are also affected by varying the above parameters.

As the propeller rotates, it is subjected to both hydrodynamic and centrifugal loadings. To keep the stress within a blade below a certain allowable level, a propeller blade must contain enough material. This acceptable stress level is affected by the material properties which are functions of steady state loading, fatigue strength, mean and unsteady blade loadings. The propeller geometric parameters, such as chord length, thickness, skew, and rake will affect the stress. The stress can be calculated approximately using simple beam theory which represents the propeller blade as a straight cantilever beam with variable cross section without camber. However, a finite element analysis is required for a more accurate analysis for the full power ahead and the backing cases.

Even for SR propellers, it is well recognized that cavitation predictions frequently do not match the measurement well. This discrepancy is mainly due to the limitations of the prediction tools. Cavitation prediction is especially complicated in the PS propulsor design because of the interactions between the rotor and the stator. Owing to the temporal and spatial variations in the velocity field of the rotor and the stator, a method which can handle the circumferential variations in the mutual interaction velocities for PS propulsors has to be developed. This is beyond the current state-of-art.

Final Design

In the final design stage, a lifting-surface theory which incorporates three -dimensional flow field effects was employed to determine the detailed blade geometry (pitch and camber distributions). In the present study, a lifting-surface program with hub image effects developed by Wang [11] is employed. Blades and their wakes are represented by vortex lattices. The hub is represented by a distribution of dipoles which ends at the hub apex. A non-zero circulation at the hub of a propulsor is set so that the normal velocity at the hub will be zero.

Though the effect of the viscous drag has been considered in the force calculations, all the design codes used in this effort are based on potential flow theory. The viscous drag has been calculated using the following empirical formula.

$$C_D = C_f(1 + 1.25(t/c) + 125(t/c)^4) \qquad (16)$$

where C_f is the skin friction coefficient for a smooth plate, and t/c is the section thickness to chord ratio. The value of C_f varies from 0.004 to 0.008 for corresponding blade section Reynolds number varying between 10^8 and 10^6.

In the design procedure, boundary layer calculations need to be performed to ensure unseparated flow along the blade. A program developed by Cebeci [12] was employed in the present study. This program can calculate incompressible laminar and turbulent boundary layers on plane and axisymmetric bodies with either smooth or rough surfaces.

Analysis

In the analysis phase, steady forces and unsteady forces and moments need to be calculated using inverse lifting-surface codes. To determine the resultant steady thrust, torque, and efficiency of the PS propulsor under design and off-design conditions, the vortex lattice method including hub effects, developed by Greeley and Kerwin [13] was employed.

Fluctuating forces and moments arise from wake nonuniformities or shaft inclination. These unsteady components can cause cavitation, strength, and radiated noise problems. In general, larger skew produces smaller vibratory forces and moments, while producing larger blade stresses. Hence, from considerations of both vibratory forces and blade stresses, the skew distribution needs to be optimized. The design is complete when the unsteady shaft forces and moments are below the design requirements. A method which can handle the variations in the mutual interaction velocities between the rotor and the stator is the key point in calculating the unsteady forces and moments for PS propulsors.

A POSTSWIRL PROPULSOR DESIGN

A PS propulsor design is presented using the method developed in the previous section. Some of the design stages will be skipped because the present design is for close-to-uniform flow.

DESIGN REQUIREMENTS

The PS propulsor was designed for close-to-uniform flow at the operating point for a surface ship. The ship speed was chosen as 20 knots (10.3 m/s). The thrust loading coefficient, C_{Th}, is 0.2871. The rotor diameter is 7.55 ft (2.30 m) and the rotation speed 199 rpm. The blade numbers of the rotor and stator are 5 and 7, respectively. The ship full power condition is 2,970 shaft horsepower (2,216 KW) per shaft.

The design parameters for the present study were chosen based on a parametric study. The stator diameter was determined through mass conservation, in Equation (2). To ensure that the stator operates inside the tip vortex of the rotor, the final stator diameter, which is 85 percent of the rotor diameter, was chosen to be slightly smaller than the preliminary diameter calculated using

mass conservation. The axial spacing was chosen to be one quarter of the rotor diameter. A summary of the design parameters for the PS propulsor is given in Table 1.

Table 1. PS propulsor design — Summary.

	Rotor	Stator
Ship Speed (knots)	20	20
Rotational Speed (rpm)	199	0
Thrust Loading Coefficient	0.2871	
Geometry		
Diameter (ft)	7.55	6.42
Number of blades	5	7
Expanded Area Ratio	0.538	0.611
Skew (deg)	25	0
Total Rake	0	0
Blade Sections	*	*
Axial Spacing (ft)	1.89	

* NACA 66 (TMB Modified) Thickness, NACA a = 0.8 Meanline

PRELIMINARY DESIGN

The lifting-line calculations will be discussed in this section. The optimum circulation distributions for the rotor and the stator are determined by the variational approach described in the previous section. The optimum and the root- and tip-unloaded circulation distributions for the rotor and stator are shown in Figure 3. The advantages of unloading the blade root and tip are to delay the blade root and tip cavitation inception and to reduce the tendency toward cavitation erosion near the blade root and tip. Since the lift coefficient at the blade root was not very high with the optimum circulation distribution, a 20 percent reduction in the blade loading at the root was made. In addition, the slope of the circulation, $\frac{d\Gamma}{dr}$, was constrained to be essentially zero at the blade root to minimize the trailing vortex sheet.

The guidelines for unloading the stator hub have to consider two factors: (1) ensure zero hub vortex strength by providing an equal and opposite total circulation at the hub with respect to the rotor, and (2) minimize the trailing vortex sheet by maintaining almost zero circulation slope at the hub.

Based on cavitation, flow separation, and efficiency considerations, the chord-length distributions of the rotor and stator were chosen. The thickness distribution was selected based on strength and cavitation considerations.

A skew distribution of 25 degrees at the tip, varying nonlinearly from zero at the hub, was selected for the rotor. The stator was designed with zero skew. The total rake for both the rotor and the stator was zero. Therefore, the rotor was given negative rake to offset the skew-induced rake.

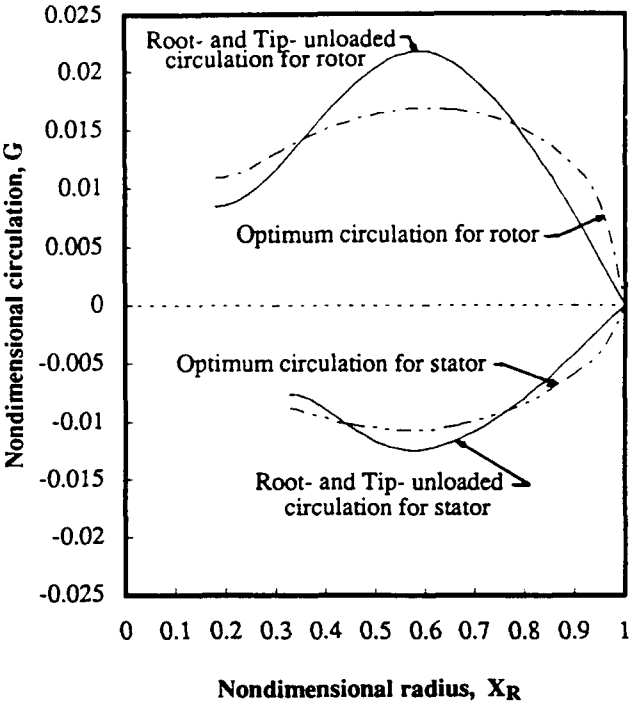

Fig. 3. Optimum and unloaded circulation distribution for rotor and stator.

INTERMEDIATE DESIGN

In the intermediate design stage, strength and cavitation was considered. The stress distributions for the rotor and stator were calculated and were determined to be well below an allowable stress of 12,500 psi maximum stress for Nickel-Aluminum-Bronze material. Although this propulsor set was designed for close-to-uniform flow, the cavitation performance of the stator is important due to the non-uniform effects of the rotor on the stator. Since there is no appropriate method to predict the cavitation for the stator, the cavitation prediction was not carried out for this design.

FINAL DESIGN

The final pitch and camber distributions were determined using lifting-surface theory with hub effects included. For marine propeller applications, an a = 0.8 meanline loading is an appropriate chordwise loading distribution from cavitation and viscous flow points of view. A NACA 66 thickness distribution was selected for the present application.

The final rotor camber and pitch distributions are shown in Figures 4 and 5 while the final stator camber and hydrodynamic pitch angle distributions are shown in Figures 4 and 6.

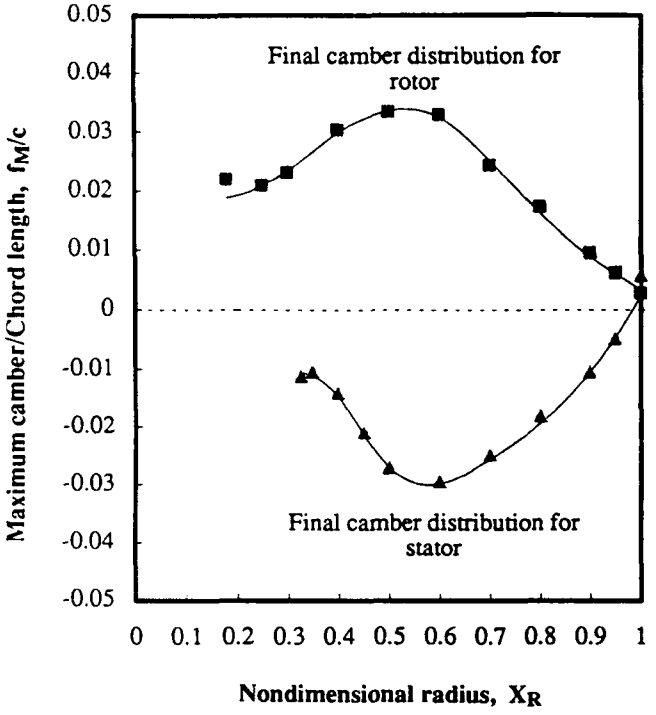

Fig. 4. Final maximum camber to chord length ratio distributions.

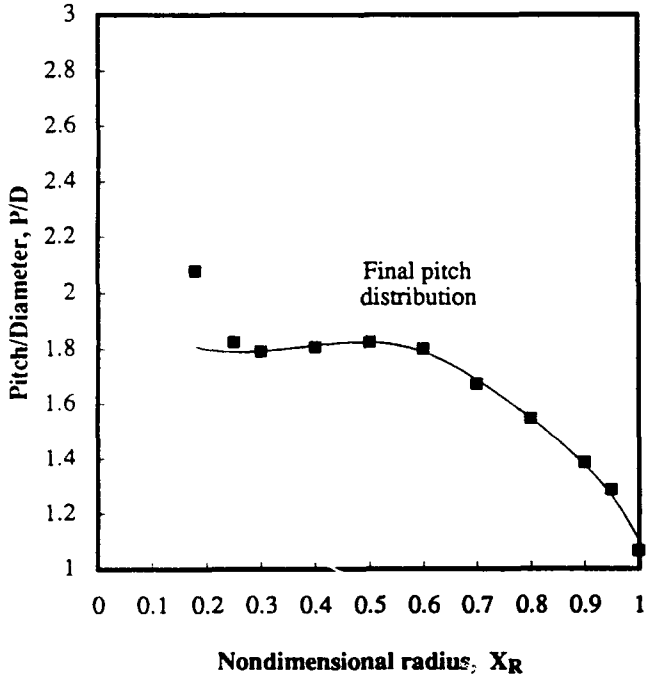

Fig. 5. Final pitch to diameter ratio for rotor.

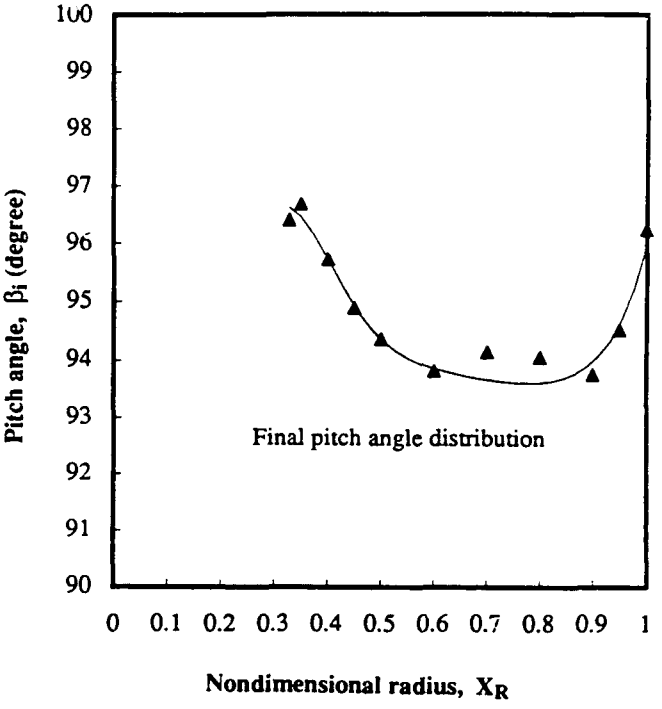

Fig. 6. Final hydrodynamic pitch angle for stator.

PERFORMANCE PREDICTION AND EXPERIMENTAL RESULTS

Aluminum models of the rotor and stator were manufactured based on the final design geometry. The self-propulsion tests were carried out using DTRC model propeller 5118 to represent the rotor and model propeller 5119 to represent the stator. The self-propulsion tests were performed at DTRC.

SELF-PROPULSION TESTS

The resistance and the self-propulsion tests for the designed PS propulsor were performed using the same ship Model 5365-A as those for the stock SR propeller. Figure 7 shows the measured delivered power and rotation speed of the unit as a function of ship speed as well as the predicted performance at the design ship speed. Table 2 also shows the predicted and measured self-propulsion performance at the design ship speed of the PS propulsor.

The effective horsepower used in the design is 4.6 percent lower than the measurement. This difference, due to the modification of the test vehicle, may cause some discrepancy between the design and the experiment. The delivered power from the prediction is 1.3 percent higher than that from the experimental values. The thrust deduction and the wake fraction estimated for the design are very close to the experimental values.

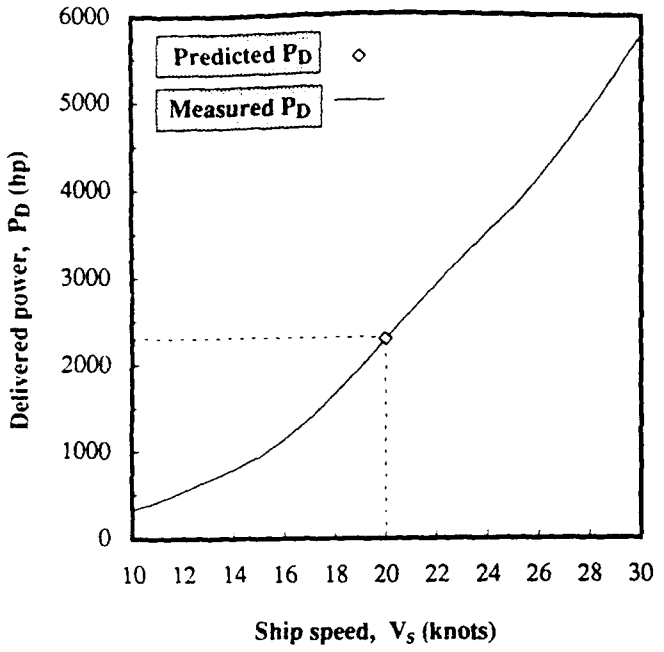

(a) Delivered power.

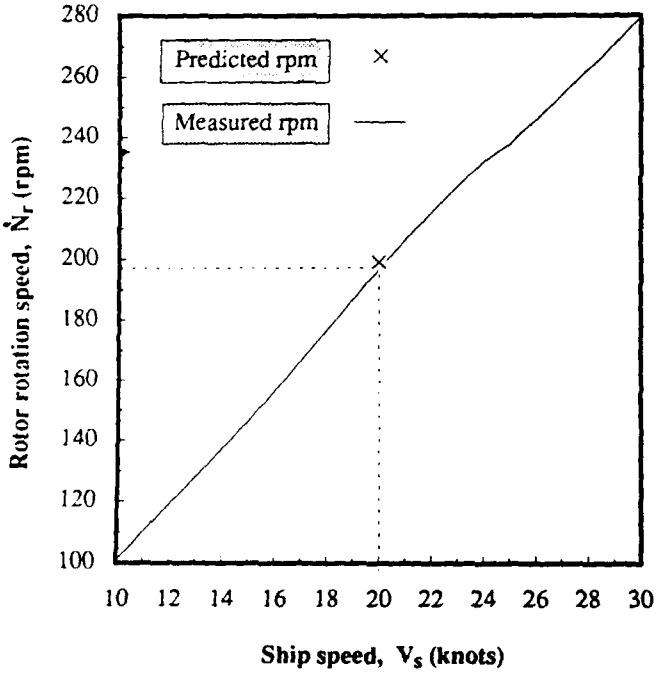

(b) Rotation speed.

Fig. 7. Predicted and measured self–propulsion test results.

Table 2. Predicted and measured powering performance of PS propulsor design.

	Prediction	Self-propulsion Experiment
V_S (knots)	20	20
P_E (hp)	1,550 (-4.6%)	1,625
P_D (hp)	2,299 (1.3%)	2,269
1-t	0.865 (-0.6%)	0.870
1-w_T	1.000 (-0.5%)	1.005
J_A	1.349 (-1.5%)	1.370
N (rpm)	199 (1.0%)	197
K_T	0.207 (-5.0%)	0.218
K_Q	0.056 (-1.8%)	0.057
η_D	0.674 (-5.7%)	0.715
η_O	0.788 (-4.5%)	0.825
η_R	1.000	1.000

The design advance coefficient is 1.5 percent lower and the predicted rotation speed is 1.0 percent higher than the measurement. The thrust and the torque predictions are 5.0 percent and 1.8 percent lower than the experiment. The predicted open water efficiency and propulsive efficiency are 4.5 percent and 5.7 percent lower than the measurement. These discrepancies are primarily due to the difference between the design and the measured effective horsepower. In general, the accuracy of the experimental measurements with the PS propulsor is ± 2 percent on thrust and torque. Overall the predicted values agree well with the experimental measurements, and in general are within the accepted accuracy of the experimental measurements. A view of the PS propulsor created on a Computer Vision system is shown in Figure 8.

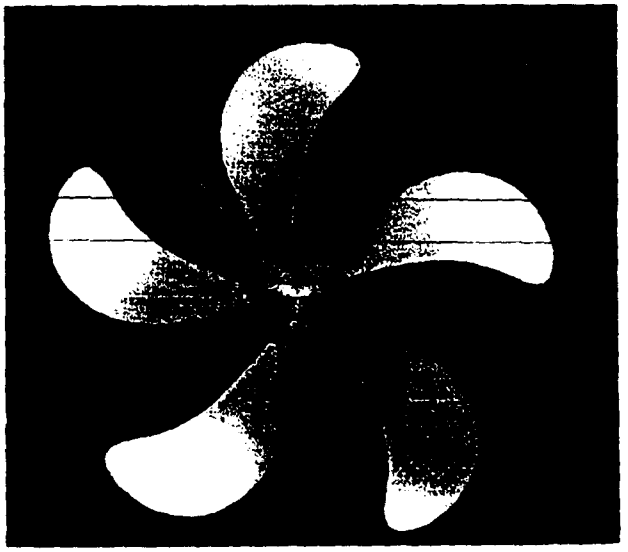

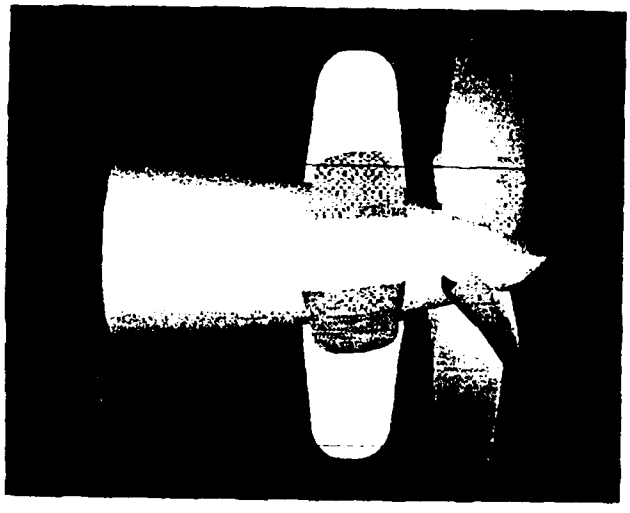

Fig. 8. A configuration of PS propulsor.

CONCLUSIONS AND RECOMMENDATIONS

The following conclusions can be drawn from the present study.

1. The present design method is an adequate procedure for the PS propulsor design. Self-propulsion experiments show that the performance predictions agree well with the experimental measurements.
2. The mutual interaction velocities between the rotor and the stator play important roles in the PS propulsor design. This is particularly important for

There are two general recommendations for future work.

1. Propulsor - hull interactions and effective wake: A method for calculating the PS propulsor - hull interactions, including thrust deduction and wake fraction, and effective wake needs to be developed. This is particularly important for the stator because the complex interactions between the PS propulsor and the hull, and the rotor and the stator.
2. Cavitation and unsteady force: A method which can handle the circumferential variations of the mutual interaction velocities between the rotor and the stator needs to be developed. This method, as a matter of fact, is crucial to the cavitation and unsteady force calculations for the stator.

ACKNOWLEDGMENT

The author would like to thank Mr. Ken Remmers and Mr. Bill Cave for carrying out the open-water and self-propulsion experiments. This work was performed for the Advanced Surface Machinery Program of Naval Surface Warfare Center under Program Element 63724N.

REFERENCES

[1] Wagner, R., "Ruckblick und Ausblick auf die Entwicklung des Contrapropellers," Jahrbuch STG, Band 30 (1929) pp. 195-256.

[2] Weinblum, G., "The Thrust Deduction," American Society of Naval Engineers, Vol. 63 (1951) pp. 363-378.

[3] Cox, B. D. and A. Hansen, "A Method for Predicting Thrust Deduction Using Propeller Lifting Surface Theory," DTNSRDC Report 77-0087, 80p. (1977).

[4] Chen, B. Y.-H. and A. M. Reed, "A Design Method and an Application for Contrarotating Propellers," 22nd American Towing Tank Conference, St. John's, Newfoundland, Canada, (1989).

[5] Huang, T., H. T. Wang, N. Santalli, and N. C. Groves, "Propeller/Stern/Boundary Layer Interaction on Axisymmetric Bodies:Theory and Experiment," DTNSRDC Report 77-0013 (1976).

[6] Shih, W.-Z., "Effective Wake Calculations by Solving the Euler Equations," Dept. of Ocean Engineering, MIT Report NO. 88-2, 66p. (1988).

[7] Kerwin, J. E., W. B. Conney and C.-Y. Hsin, "Optimum Circulation Distributions for Single and Multiple-Component propulsors," 21st American Towing Tank Conference, Washington D.C., (1986).

[8] Caster, E., J. A. Diskin, and T. A. Lafone," A Lifting Line Computer Program for Preliminary Design of Propellers," DTNSRDC Ship Performance Department Report, DTNSRDC/SPD-595-01 (1975).

[9] Chen, B. Y.-H., A. M. Reed, and K.-H. Kim, "A Vane Wheel Propulsor for A Naval Auxiliary" Symposium on Hydrodynamic Performance Enhancement for Marine Applications, NUSC, Newport, RI, (1988).

[10] Chen, B. Y.-H. and A. M. Reed, "A lifting Surface Program for Contrarotating Propellers," Symposium on Hydrodynamic Performance Enhancement for Marine Applications, NUSC, Newport, RI, (1988).

[11] Wang, M. H., "Hub Effects in Propeller Design and Analysis," Department of Ocean Engineering, MIT Report 85-14 (1985).

[12] Cebeci, T., " A Computer Program for Calculating Incompressible Laminar and Turbulent Boundary Layers on Plane and Axisymmetric Bodies with Surface Roughness," Report No. TR-78-1, Dept. of Mechanical Engineering, California State University at Long Beach, Long Beach, CA (1978).

[13] Greeley, D. S. and J. E. Kerwin, "Numerical Methods for Propeller Design and Analysis in Steady Flow, "Transactions SNAME, Vol. 90 (1982).

THIS PAGE INTENTIONALLY LEFT BLANK

APPENDIX

Parametric Studies

The purpose of this study is to secure an optimum design for a PS propulsor through parametric studies. The lifting-line theory developed by Kerwin et al. as in reference (7) was employed. The parametric studies covered the following range of parameters.

- Rotor diameter, D_r, 6.5 - 8.0 ft (1.98 - 2.44 m).
- Rotor rotation speed, N_r, 150 - 210 rpm.
- Ratio of stator and rotor diameter, D_s/D_r, 0.85 - 0.95

As shown in Figure 9, although the selected rotor diameter, 7.55 ft (2.30 m), is not the optimum diameter, the difference of the propulsive efficiency between the optimum and the selected diameters is around 0.3 point.

Figure 10 shows that the selected rotor rotation speed, 199 rpm, is not the optimum rotation speed. However, the difference of the propulsive efficiency between the optimum and the selected rotation speeds is small.

The optimum rotor diameter and rotor rotation speed were calculated only based on the consideration of efficiency. However, the selected rotor and rotation speed were calculated based on consideration not only of efficiency but of cavitation, strength, and flow separation. Therefore, there is a slight difference between the optimum and selected rotor diameter and rotation speed.

Figure 11 indicates that the propulsive efficiency is insensitive to the ratio of the stator and rotor diameters. Since lifting-line theory does not account for mass conservation between the rotor and stator, additional consideration must be included.

The basic guideline for determining the final stator diameter is to ensure that the rotor tip vortices will not impinge on the stator blades because they can result in erosion or blade rate noise of the stator. To be on the safe side, the final stator diameter, was selected to be 85 percent of the rotor diameter. This is slightly smaller than the rotor slipstream diameter calculated using mass conservation. As seen in Figure 11, there is almost no change in efficiency with varying the ratio of the stator diameter to the rotor diameter. In other words, there is no penalty in efficiency to select this specific stator diameter. The axial spacing was chosen to be one quarter of the rotor diameter.

Geometric Specification

Based on cavitation, flow separation, and efficiency considerations, the chord-length distributions of the rotor and stator were chosen. The chord distributions for the rotor and stator are shown in Figure 12. The expanded area ratio (EAR) was calculated based on both Burrill's and Keller's criteria for cavitation inception.

The thickness distribution was selected based on strength and cavitation considerations. Figure 13 shows the thickness distributions for the rotor and stator.

As shown in Figure 14 , a tip skew distribution of 25 degrees, varying nonlinearly from zero at the hub, was selected for the rotor. The stator was designed with zero skew. The total rake for both rotor and stator was zero. Therefore, the rotor has negative rake to offset the skew-induced rake. The stress distributions computed by beam theory corresponding to these choices of geometry are given in Figure 15.

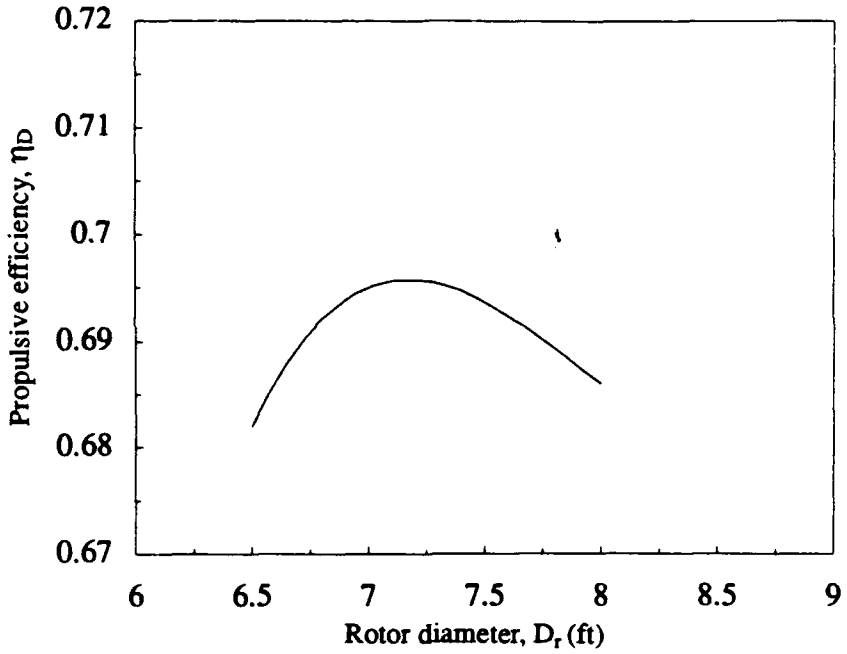

Fig. 9. Propulsive efficiency versus rotor diameter for fixed rotor rotation speed and ratio of stator and rotor diameter.

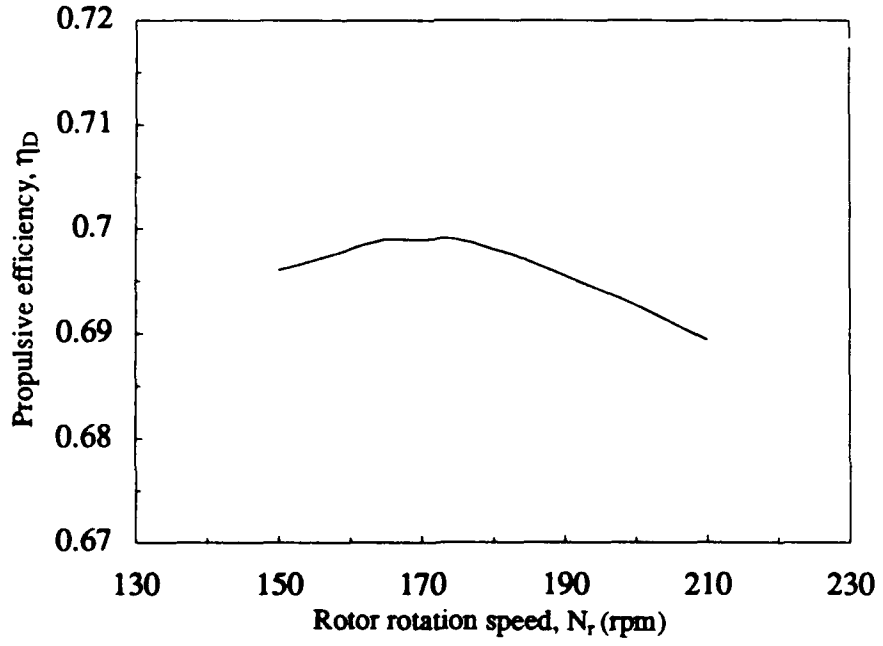

Fig. 10. Propulsive efficiency versus rotor rotation speed for fixed rotor diameter and ratio of stator and rotor diameter.

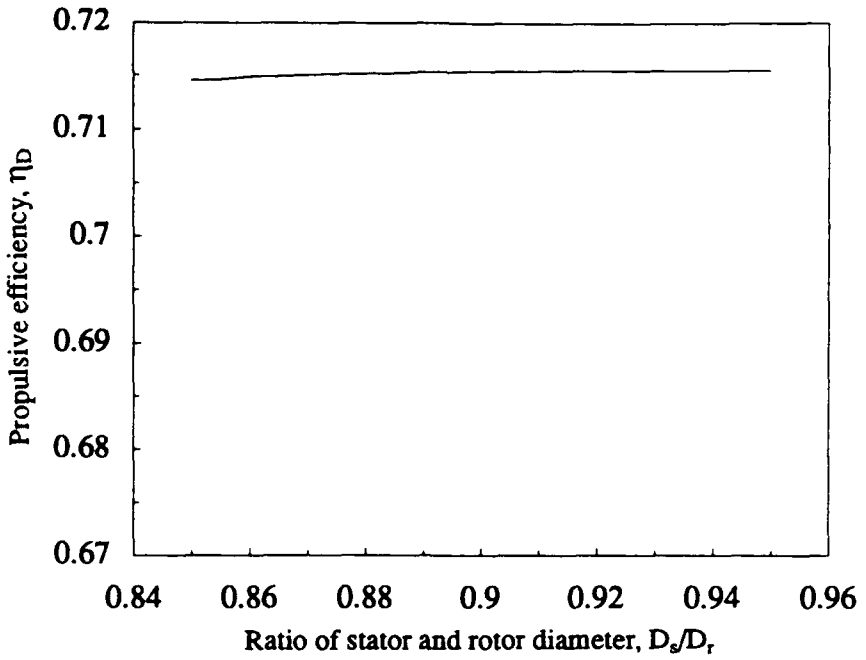

Fig. 11. Propulsive efficiency versus ratio of stator and rotor diameter for fixed rotor diameter and rotation speed.

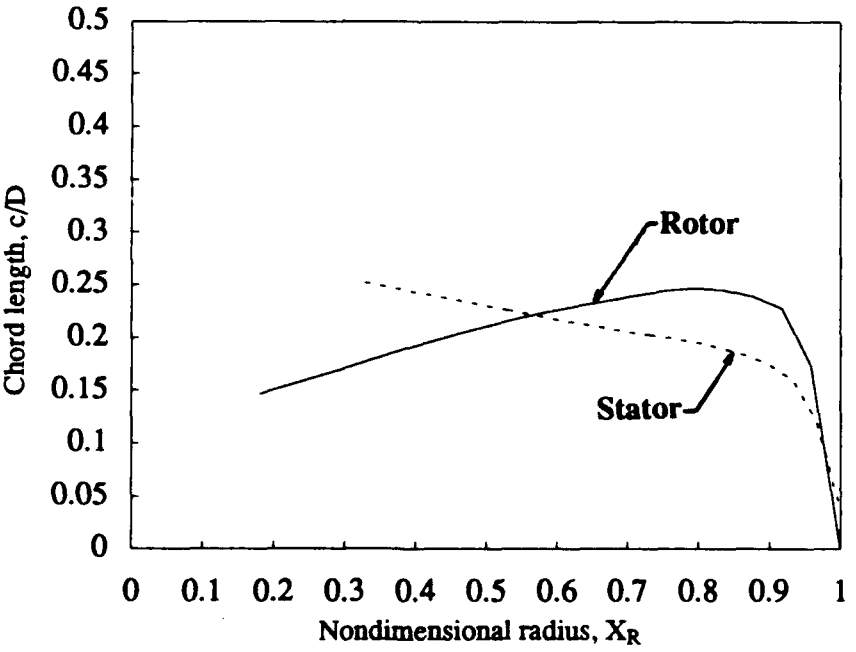

Fig. 12. Radial distribution of chord length.

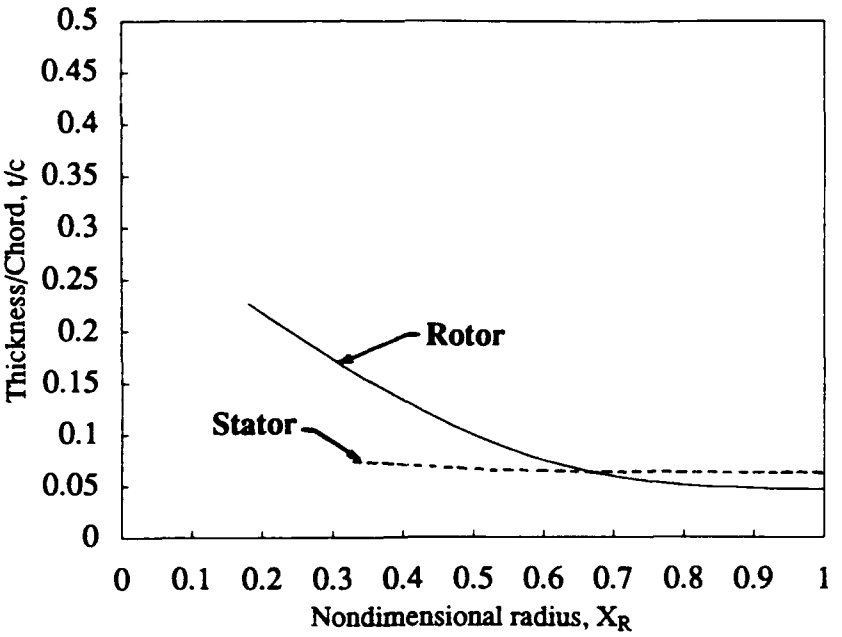

Fig. 13. Radial distribution of thickness.

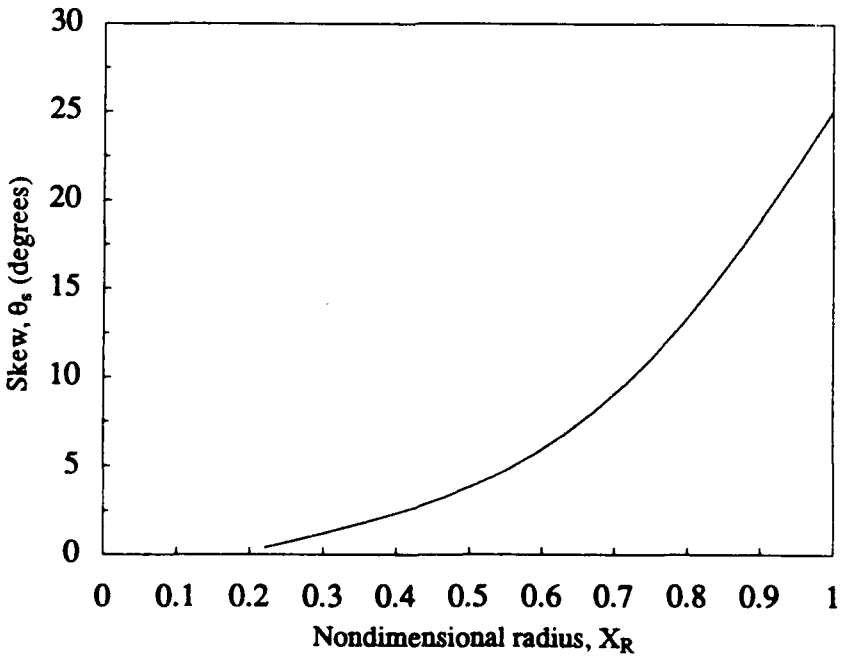

Fig. 14. Radial distribution of skew.

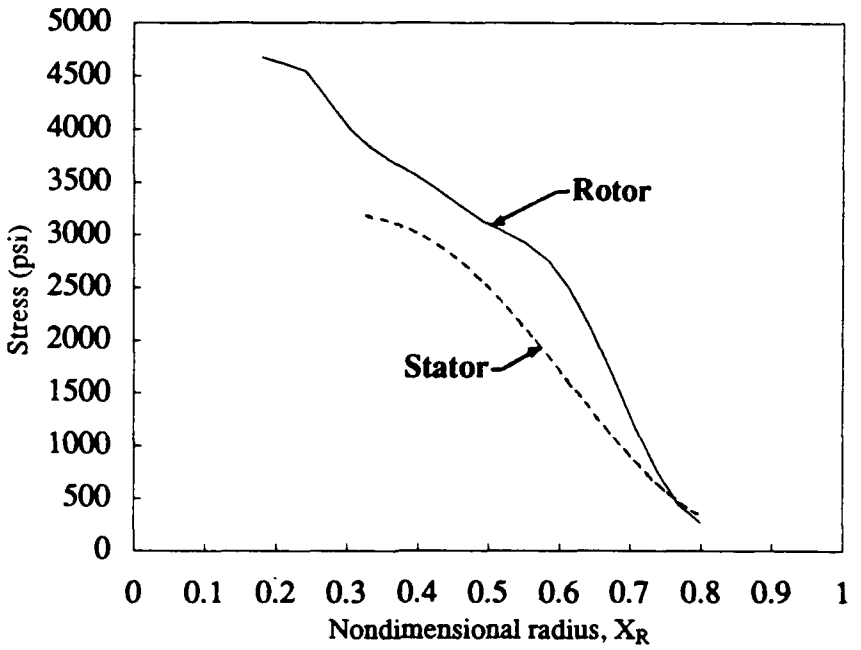

Fig. 15. Radial distribution of stress.

Final Postswirl Propulsor Geometry

The final geometric specifications of the PS propulsor, including the details of the leading and trailing edges were computed using the computer code, XYZ-PROP, developed by Brockett.* All the input data, such as the chord length, thickness, skew, pitch and camber distributions, were faired by a cubic spline procedure before being input to XYZ-PROP. A list of the chord length, thickness, skew, pitch and camber distributions are given in Table 3.

Table 3. Final design geometry for PS propulsor.

a. Rotor.

r/R	c/D	P/D	i_T/D	θ_s	t/c	f_m/c
0.1800	0.14603	1.8075	0.0000	0.00000	0.22702	0.01876
0.2500	0.16030	1.7875	0.0000	0.67623	0.19527	0.02084
0.3000	0.17084	1.7909	0.0000	1.18209	0.17324	0.02336
0.4000	0.19178	1.8125	0.0000	2.31700	0.13278	0.02978
0.5000	0.21059	1.8244	0.0000	3.76256	0.09916	0.03360
0.6000	0.22638	1.7875	0.0000	5.87000	0.07453	0.03250
0.7000	0.23900	1.6875	0.0000	8.99300	0.05885	0.02519
0.8000	0.24709	1.5463	0.0000	13.31010	0.05067	0.01632
0.9000	0.23416	1.3750	0.0000	18.82284	0.04747	0.00879
0.9500	0.19326	1.2625	0.0000	21.86989	0.04681	0.00595
1.0000	0.00000	1.1000	0.0000	25.00000	0.04635	0.00342

b. Stator.

r/R	c/D	P/D	i_T/D	θ_s	t/c	f_m/c
0.3281	0.25156	96.6220	0.0000	0.0000	0.07459	-0.01055
0.3500	0.24893	96.4790	0.0000	0.0000	0.07328	-0.01100
0.4000	0.24278	95.7450	0.0000	0.0000	0.07046	-0.01478
0.4500	0.23647	94.9375	0.0000	0.0000	0.06811	-0.02145
0.5000	0.23009	94.3715	0.0000	0.0000	0.06625	-0.02674
0.6000	0.21751	93.8499	0.0000	0.0000	0.06380	-0.02990
0.7000	0.20585	93.6830	0.0000	0.0000	0.06273	-0.02596
0.8000	0.19524	93.6510	0.0000	0.0000	0.06249	-0.01940
0.9000	0.17476	94.0000	0.0000	0.0000	0.06286	-0.01053
0.9500	0.14502	94.6250	0.0000	0.0000	0.06324	-0.00469
1.0000	0.03795	95.9800	0.0000	0.0000	0.06369	0.00223

* Brockett, T. E. 1976. Analytical Specification of Propeller Blade-Surface Geometry. DTRC Ship Hydrodynamics Department Report, DTRC/SHD-699-01.

INITIAL DISTRIBUTION

Copies

- 3 CNO
  - 1 222
  - 1 22T
  - 1 23B
- 2 ONT
  - 1 21 E. Zimet
  - 1 211 J. Gagorik
- 1 OAT/ 30 J. DeCorpo
- 1 ONR/ 113
- 1 ONR Boston
- 1 ONR Chicago
- 1 ONR London, England
- 1 NRL
- 2 USNA
  - 1 Lib
  - 1 Johnson
- 1 NAVPGSCOL Lib
- 1 NROTC & NAVADMINU, MIT
- 1 NADC
- 1 NOSC/ Mautner
- 1 NSWC
- 1 NUSC/ 01V
- 9 NAVSEA
  - 1 501
  - 1 503
  - 1 5112
  - 1 55N2
  - 1 55W32
  - 1 56X1
  - 2 56X7
  - 1 PMRS 330/ M. Finnerty

Copies

- 2 MMA
  - 1 Lib
  - 1 Maritime Res Cen
- 12 DTIC
- 2 HQS COGARD
- 1 US Coast Guard (G–ENE–4A)
- 1 LC/SCI & Tech Div
- 2 NASA STIF
  - 1 Dir Res
- 1 NSF Engr Div/Lib
- 1 DOT Lib
- 2 U. Cal Berkley
  - 1 Lib
  - 1 Webster
- 1 U. Mississippi, Dept. of M.E.
  - 1 Fox
- 3 CIT
  - 1 AERO Lib
  - 1 Acosta
  - 1 Wu
- 4 U. Iowa
  - 1 Lib
  - 1 IHR/Kennedy
  - 1 IHR/Stern
  - 1 IHR/Patel
- 3 U. Michigan
  - 1 Lib
  - 1 Parsons
  - 1 Vorus
- 3 MIT
  - 1 Barker Engr Lib
  - 2 Ocean Engr/Kerwin

INITIAL DISTRIBUTION (Continued)

Copies

- 3 State U. Maritime Coll
  - 1 ARL Lib
  - 1 Engr Dept
  - 1 Inst Math Sci
- 4 Penn State U. APL
  - 1 Lib
  - 1 M. Billet
  - 1 Gearhart
  - 1 Thompson
- 1 Boeing Adv Amr Sys Div
- 1 BB&N/ Jackson
- 1 Brewer Engr Lab
- 1 Cambridge Acous/ Junger
- 1 Calspan, Inc./ Ritter
- 1 Stanford U/ Ashley
- 1 Stanford Res Inst Lib
- 2 Sit Davidson Lab
  - 1 Lib
  - 1 Savitski
- 1 Texas U. ARL Lib
- 1 Utah State U./ Jeppson
- 2 VPI/ Dept Aero & Ocean Engr
  - 1 Schetz
  - 1 Kaplan
- 2 Webb Inst
  - 1 Ward
  - 1 Hadler
- 1 WHOI Ocean Engr Dept
- 1 WPI Alden Hydr Lab Lib

Copies

- 1 ASME/ Res Comm Info
- 1 ASNE
- 1 SNAME/ Tech Lib
- 1 AERO Jet–General/ Beckwith
- 1 Allis Chalmers, York, PA
- 1 AVCO Lycoming
- 1 Baker Manufacturing
- 2 Bird–Johnson Co
  - 1 Norton
  - 1 Platzer
- 1 Douglas Aircraft/ Lib
- 2 Exxon Res Div
  - 1 Lib
  - 1 Fitzgerald
- 1 Friede & Goldman/ Michel
- 1 General Dynamics, EB/ Boatwright
- 1 Gibbs & Cox/ Lib
- 1 Rosenblatt & Son/ Lib
- 1 Grumman Aerospace/ Carl
- 1 Ingalls Shipbuilding
- 1 Inst for Defense Anal
- 1 Itek Vidya
- 1 Lips Duran/ Kress
- 1 Littleton R & Engr Corp/ Reed
- 1 Litton Industries
- 1 Lockheed, Sunnyvale/ Waid

INITIAL DISTRIBUTION (Continued)

Copies		Copies	Code	Name
2	McDonnel Douglas, Long Beach	1	15	Morgan
	1 Cebeci	1	1506	Walden
	1 Hess	1	1508	Boswell
1	Maritech, Inc./ Vassilopoulis	1	152	Lin
2	HRA/JJMA, Inc.	1	1521	Day
	1 Cox	1	1521	Karafiath
	1 Scherer	1	1522	Remmers
1	Arete Associates/ Brockett	1	1522	Wilson
1	Nielson Engr/ Spangler	1	154	McCarthy
1	NKF Associates/ Noonan	1	1541	Yim
1	NAR Space/ Ujihara	1	1542	Huang
2	Atlantic Applied Research	20	1544	Chen
	1 Brown	1	156	Cieslowski
	1 Greeley	1	17	Krenzke
1	Propulsion Dynamics, Inc.	1	1720	Rockwell
1	Sperry Sys Mgmt Lib/ Shapiro	1	19	Sevik
1	OF Technologies/ Furuya	1	1901	Strasberg
1	UA Hamilton Standard/ Cornell	1	1905.1	Blake
1	Clarkson U./ Valentine	1	1906	Vendittis
		1	1941	Kilcullen
		1	1944	Mathews
		2	27B	Duvall
		1	3411	Publications
		1	342.1	TIC (C)
		1	342.2	TIC (A)
		10	3432	Reports Control

CENTER DISTRIBUTION

Copies	Code	Name
1	011	Chaplin
1	0113	Winegrad
1	0117	Nakonechny

THIS PAGE INTENTIONALLY LEFT BLANK